Journal of Biomechanics 43 (2010) 1835–1839

Contents lists available at ScienceDirect

Journal of Biomechanics

journal homepage: www.elsevier.com/locate/jbiomech
www.JBiomech.com

Short communication

A fast quadrature-based numerical method for the continuous spectrum biphasic poroviscoelastic model of articular cartilage

Michael Stuebner, Mansoor A. Haider *

Department of Mathematics, North Carolina State University, Box 8205, Raleigh, NC 27695-8205, USA

ARTICLE INFO

Article history:
Accepted 12 February 2010

Keywords:
Collagen
Proteoglycan
Stress relaxation
Discrete spectrum

ABSTRACT

A new and efficient method for numerical solution of the continuous spectrum biphasic poroviscoelastic (BPVE) model of articular cartilage is presented. Development of the method is based on a composite Gauss–Legendre quadrature approximation of the continuous spectrum relaxation function that leads to an exponential series representation. The separability property of the exponential terms in the series is exploited to develop a numerical scheme that can be reduced to an update rule requiring retention of the strain history at only the previous time step. The cost of the resulting temporal discretization scheme is $O(N)$ for N time steps. Application and calibration of the method is illustrated in the context of a finite difference solution of the one-dimensional confined compression BPVE stress-relaxation problem. Accuracy of the numerical method is demonstrated by comparison to a theoretical Laplace transform solution for a range of viscoelastic relaxation times that are representative of articular cartilage.

1. Introduction

In modeling viscoelastic deformation of articular cartilage, the consideration of both flow-dependent and flow-independent dissipation mechanisms necessitates the use of a linear biphasic poroviscoelastic (BPVE) model (Mak, 1986). Intrinsic dissipation in cartilage extracellular matrix is represented using a constitutive law in which stress depends on the strain history via a hereditary integral with a continuous relaxation spectrum (Fung, 1993), and BPVE models have been used to analyze cartilage viscoelasticity in a variety of settings (Desmarais and Aissaoui, 2008; DiSilvestro and Suh, 2001, 2002; Setton et al., 1993). Direct solution of the BPVE governing equations can be costly due to the dependence of the current solution on the entire strain history. Commonly, a discrete spectrum approximation is used to approximate the continuous spectrum relaxation function. This technique has a key advantage in that the exponential terms in the discrete spectrum series are separable functions, leading to an update rule that requires retention of the strain history at only the previous time step. However, accurate reproduction of the continuous spectrum relaxation function using an exponential series can be difficult to achieve and parameters in the representation can be non-unique (Fung, 1993).

An alternate approach is to use analytical properties of the continuous spectrum constitutive law to derive new approximations that can accelerate numerical solution of the BPVE model. In a prior study (Haider and Schugart, 2006), integration by parts was used to develop an alternate BPVE formulation with an error estimate that enabled retention of a fixed portion of the strain history without loss of accuracy. While exhibiting a significant cost reduction relative to direct solution of the continuous spectrum BPVE model, the cost was still much greater than discrete spectrum BPVE models. In this study, we present a new quadrature-based method for the BPVE model that has computational efficiency similar to BPVE models based on a discrete spectrum approximation while, simultaneously, exhibiting accuracy comparable to the continuous spectrum BPVE model.

2. Methods

2.1. 1D BPVE model

We illustrate our numerical method in the context of a finite difference solution of the one-dimensional (1D) confined compression BPVE stress relaxation problem in the range of infinitesimal strain. In this case, an analytical Laplace transform solution is available for comparison (Mak, 1986). The 1D BPVE model can be reduced to

$$\frac{1}{\kappa}\frac{\partial u}{\partial t} = \frac{\partial \sigma}{\partial z}, \quad 0 < z < h,\ 0 < t < t_f, \tag{1}$$

where $u(z,t)$ is the axial (z) displacement, h is the cylindrical sample height. κ is the hydraulic permeability and t_f denotes the duration of the experiment. In (1) σ represents the axial normal stress, i.e. $\sigma = \sigma_{zz}$, and is viscoelastic:

$$\sigma(z,t) = H_A \int_{-\infty}^{t} G(t-\tau)\frac{\partial}{\partial \tau}\left(\frac{\partial u}{\partial z}(z,\tau)\right) d\tau, \tag{2}$$

* Corresponding author. Tel.: +1 919 515 3100; fax: +1 919 515 3798.
E-mail address: m_haider@ncsu.edu (M.A. Haider).

0021-9290/$ - see front matter © 2010 Elsevier Ltd. All rights reserved.
doi:10.1016/j.jbiomech.2010.02.023

where H_A is the "drained" aggregate modulus of the solid phase and $G(t)$ is the reduced relaxation function (Fung, 1993). For articular cartilage, as well as many other soft tissues, a continuous spectrum relaxation function is employed (Fung, 1993; Neubert, 1963):

$$G(t) = 1 + c\int_{\tau_1}^{\tau_2} \frac{e^{-t/s}}{s}\, ds. \tag{3}$$

Typically, the relaxation times τ_1 and τ_2 in (3) are separated by several orders of magnitude.

2.2. Discrete spectrum approximation and separability

The computational cost for direct temporal discretization of (1)–(3) with N time steps is $O(N^2)$, due to the history dependence in the viscoelastic constitutive law (2). The discrete spectrum approximation of (3) is written as

$$G(t) \approx G^{DS}(t) \equiv G_\infty + \sum_{i=0}^{N_{DS}} G_i K_i^{DS}(t),$$
$$\text{where } K_i^{DS}(t) = e^{-t/v_i}, i = 0, \ldots, N_{DS}. \tag{4}$$

In (4), G_i are discrete moduli, v_i are discrete relaxation times and $G_\infty = 1$. For this approximate BPVE model, nonuniqueness in the representation (4) can be addressed by assuming that $G_i = \overline{G} \equiv (G_0 - 1)/(N_{DS}+1)$, where $G_0 = G_{DS}(0) = G_\infty + \sum_{i=0}^{N_{DS}} G_i$, and by assigning v_i with values that are equally distributed, on a logarithmic scale, in the interval between τ_1 and τ_2 (Suh and Bai, 1998). The result is an approximate model (4) that has the same number of parameters as the continuous spectrum model (3), but with a significant loss in accuracy. Numerical solutions of (1), (2), in which (3) has been approximated by (4), have the separability property, i.e. $K_i^{DS}(t+r) = e^{-r/v_i} K_i^{DS}(t)$. Specifically, in a time-marching scheme with time step Δt, it follows from (4) that:

$$G^{DS}(t+\Delta t) \equiv G_\infty + \sum_{i=0}^{N_{DS}} G_i K_i^{DS}(t+\Delta t) = G_\infty + \sum_{i=0}^{N_{DS}} G_i e^{-\Delta t/v_i} K_i^{DS}(t), \tag{5}$$

thus yielding an update rule for the relaxation function that can be exploited to reduce cost for numerical solution of (1) from $O(N^2)$ to $O(N)$ in time (see, e.g., Suh and Bai (1998)).

2.3. A new quadrature-based formulation

A disadvantage of the approximation (4) is that accuracy in representation of (3) is difficult to achieve without the introduction of a significant number of additional parameters. We now demonstrate that the integral in (3) can also be represented via an exponential series based on Gauss–Legendre quadrature, and also has the separability property described in Section 2.2. Consider an equal partition, in the logarithmic sense, of the interval $[\tau_1, \tau_2]$ with $N_{int}+1$ partition points $\{s_j\}_{j=0}^{N_{int}}$ given by $s_j = \tau_1^{1-j/N_{int}} \tau_2^{j/N_{int}}$ $(j = 0, \ldots, N_{int})$. Denote the length of the j th subinterval by l_j. On the j th sub-interval $[s_{j-1}, s_j]$ $(j = 1, \ldots, N_{int})$, introduce N_Q points $s_{jk} = s_{j-1} + \frac{l_j}{2}(\xi_k + 1)$, $(k = 1, \ldots, N_Q)$, where ξ_k correspond to the abscissas for N_Q-point Gauss–Legendre quadrature on the standard interval $[-1, 1]$, with corresponding weights w_k. Based on these definitions, the composite Gauss–Legendre quadrature approximation of the continuous spectrum relaxation function in (3) is

$$G(t) = 1 + c\int_{\tau_1}^{\tau_2} \frac{e^{-t/s}}{s} ds \approx G^Q(t) \equiv 1 + c\sum_{j=1}^{N_{int}} \frac{l_j}{2} \sum_{k=1}^{N_Q} \frac{w_k}{s_{jk}} K_{jk}^Q(t)$$
$$\text{where } K_{jk}^Q(t) = e^{-t/s_{jk}}. \tag{6}$$

Since (6) is an exponential series, the separability property of $K_{jk}^Q(t)$, i.e. $K_{jk}^Q(t+r) = e^{-r/s_{jk}} K_{jk}^Q(t)$, can be used to write

$$G^Q(t+\Delta t) \equiv 1 + c\sum_{j=1}^{N_{int}} \frac{l_j}{2} \sum_{k=1}^{N_Q} \frac{w_k}{s_{jk}} K_{jk}^Q(t+\Delta t) = 1 + c\sum_{j=1}^{N_{int}} \frac{l_j}{2} \sum_{k=1}^{N_Q} \frac{w_k}{s_{jk}} e^{-\Delta t/s_{jk}} K_{jk}^Q(t). \tag{7}$$

Eq. (7) provides an update rule that can be used to develop a numerical solution of (1) that is $O(N)$ in time in that it requires retention of the strain history at only the previous time step. The primary advantage of our new formulation is that it derives an exponential series approximation of the continuous spectrum relaxation function (3) via Gauss–Legendre quadrature, thus increasing the potential for maximizing accuracy while, simultaneously, minimizing computational cost.

2.4. Discretization and implementation

The temporal discretization scheme described in Section 2.3 is developed in the case where the governing equations are nondimensionalized by taking h as the

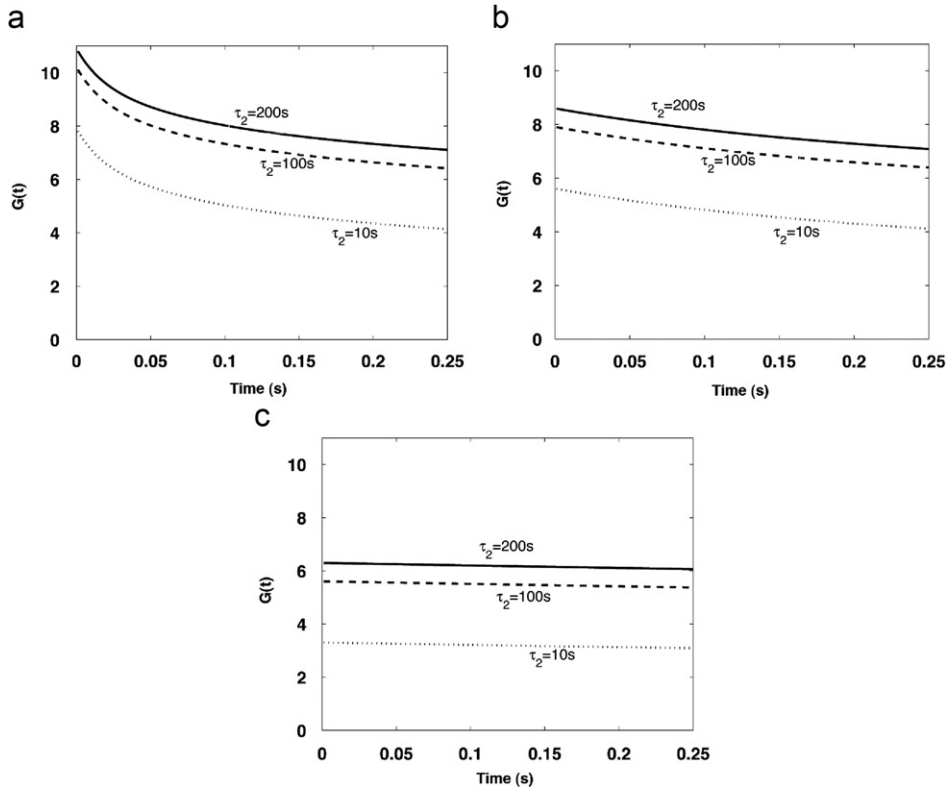

Fig. 1. The reduced relaxation function $G(t)$ shown on the domain $[0, \Delta t]$ of the error measure $E(t)$ in (13) for the nine cases considered: (a) $\tau_1 = 0.01$ s, (b) $\tau_1 = 0.1$ s, (c) $\tau_1 = 1$ s.

unit of length, the biphasic gel relaxation time $h^2/(\kappa H_A)$ (Mow et al., 1980) as the unit of time, and H_A as the unit of stress. Assuming no external loading for $t<0$, and letting $v=\partial u/\partial t$, the governing Eqs. (1) and (2) are approximated, using our quadrature based relaxation function (6), as

$$v(z,t)=\int_0^t G^Q(t-\tau)\frac{\partial^2 v}{\partial z^2}(z,\tau)\,d\tau,\quad 0<z<1,\ 0<t<\frac{\kappa H_A}{h^2}t_f. \tag{8}$$

Introduce $z_m=m\Delta z$, $m=0\ldots M$, where $\Delta z=1/M$ and $t_n=n\Delta t$, $n=0\ldots N$, where $\Delta t=\frac{\kappa H_A}{h^2}\frac{t_f}{N}$, and let $v_m^n\equiv v(z_m,t_n)$. Using (6) in (8), the solution after one time step is

$$v_m^1=\int_0^{\Delta t}\frac{\partial^2 v}{\partial z^2}(z,\tau)\,d\tau+c\sum_{j=1}^{N_{int}}\sum_{k=1}^{N_Q} I_{jk}(z,\Delta t),$$
$$\text{where } I_{jk}(z,t)\equiv\int_0^t \frac{l_j}{2}\frac{w_k}{s_{jk}}K_{jk}^Q(t-\tau)\frac{\partial^2 v}{\partial z^2}(z,\tau)\,d\tau \tag{9}$$

For later times ($n=1,2,\ldots,N$), we write

$$v_m^{n+1}=\int_0^{(n+1)\Delta t}\frac{\partial^2 v}{\partial z^2}(z,\tau)d\tau+c\sum_{j=1}^{N_{int}}\sum_{k=1}^{N_Q} I_{jk}(z,(n+1)\Delta t). \tag{10}$$

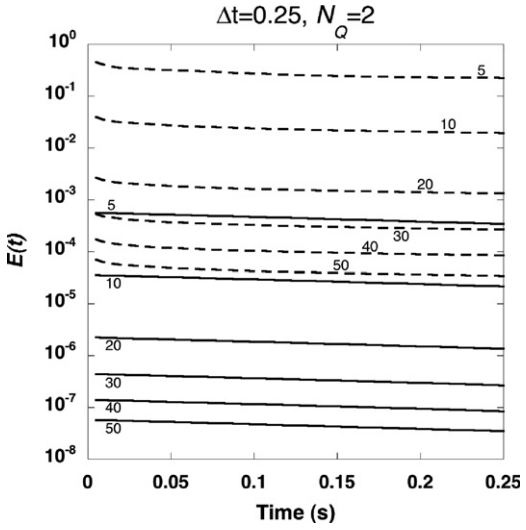

Fig. 2. Illustration of error measure $E(t)$ in (13) for calibration of the number of quadrature intervals N_{int}. For the range of material parameters considered, the best case $\tau_1=1.0$ s, $\tau_2=10$ s (solid) and the worst case $\tau_1=0.01$ s, $\tau_2=200$ s (dashed) are shown. Numbers on curves indicate the value of N_{int} for each case considered.

Due to the separability property of $K_{jk}^Q(t)$, we can derive the following update rule ($n=1,2,\ldots,N$)

$$\begin{aligned}I_{jk}(z,(n+1)\Delta t)&=\int_0^{(n+1)\Delta t}\frac{l_j}{2}\frac{w_k}{s_{jk}}K_{jk}^Q((n+1)\Delta t-\tau)\frac{\partial^2 v}{\partial z^2}(z,\tau)\,d\tau\\&=\int_0^{n\Delta t}\frac{l_j}{2}\frac{w_k}{s_{jk}}K_{jk}^Q(n\Delta t-\tau+\Delta t)\frac{\partial^2 v}{\partial z^2}(z,\tau)\,d\tau\\&\quad+\int_{n\Delta t}^{(n+1)\Delta t}\frac{l_j}{2}\frac{w_k}{s_{jk}}K_{jk}^Q(n\Delta t-\tau+\Delta t)\frac{\partial^2 v}{\partial z^2}(z,\tau)d\tau\\&=e^{-\Delta t/s_{jk}}\int_0^{n\Delta t}\frac{l_j}{2}\frac{w_k}{s_{jk}}K_{jk}^Q(n\Delta t-\tau)\frac{\partial^2 v}{\partial z^2}(z,\tau)\,d\tau\\&\quad+\int_{n\Delta t}^{(n+1)\Delta t}\frac{l_j}{2}\frac{w_k}{s_{jk}}K_{jk}^Q(n\Delta t-\tau+\Delta t)\frac{\partial^2 v}{\partial z^2}(z,\tau)\,d\tau.\end{aligned} \tag{11}$$

Using the definition of $I_{jk}(z,t)$ from (9) in (11), we obtain

$$I_{jk}(z,(n+1)\Delta t)=e^{-\Delta t/s_{jk}}I_{jk}(z,n\Delta t)+\int_{n\Delta t}^{(n+1)\Delta t}\frac{l_j}{2}\frac{w_k}{s_{jk}}K_{jk}^Q(n\Delta t-\tau+\Delta t)\frac{\partial^2 v}{\partial z^2}(z,\tau)\,d\tau.$$

Via the transformation $\tilde{\tau}=\tau-n\Delta t$, the integral in the last expression can be transformed to yield the following update rule ($n=1,2,\ldots,N$):

$$I_{jk}(z,(n+1)\Delta t)=e^{-\Delta t/s_{jk}}I_{jk}(z,n\Delta t)+\int_0^{\Delta t}\frac{l_j}{2}\frac{w_k}{s_{jk}}K_{jk}^Q(\Delta t-\tilde{\tau})\frac{\partial^2 v}{\partial z^2}(z,n\Delta t+\tilde{\tau})\,d\tilde{\tau}, \tag{12}$$

which requires retention of the strain history at only the previous time step.

Based on this new approach to temporal discretization, we obtain a numerical scheme that is $O(N)$ with respect to time and consists of Eqs. (9), (10) and (12). The scheme is complete once a spatial operator (e.g. based on finite differences or finite elements) is chosen for approximating $\partial^2 v/\partial z^2$, an integration rule is chosen for approximating the time integrals, and initial and boundary conditions are prescribed. In our implementation, (second order) central finite differences were used in space and the trapezoidal rule was used for time integration. The resulting scheme leads to a tridiagonal linear system for rapid solution of $v_m^n, m=1,\ldots,M$ at each time step n. Displacements u_m^n are recovered from velocities v_m^n via the update rule $u_m^n=u_m^{n-1}+\frac{1}{2}(v_m^n+v_m^{n-1})\Delta t$, $n=1,\ldots,N$.

3. Results

Viscoelastic relaxation times in (3) were considered for the cases $\tau_1=0.01,0.1,1.0$ s and $\tau_2=10,100,200$ s with c=1. Based on mean parameter values from DiSilvestro and Suh (2001), material and geometric parameters were set as H_A=1.29 MPa, $\kappa=1.72\times10^{-15}$ m^4/(Ns) and h=1.28 mm. In their study, mean values of short- and long-term relaxation times in $G^{DS}(t)$ were reported as 0.62 and 85.1 s, respectively.

For a particular strain history, it is evident that accuracy of our numerical scheme (9), (10) and (12) depends on the following

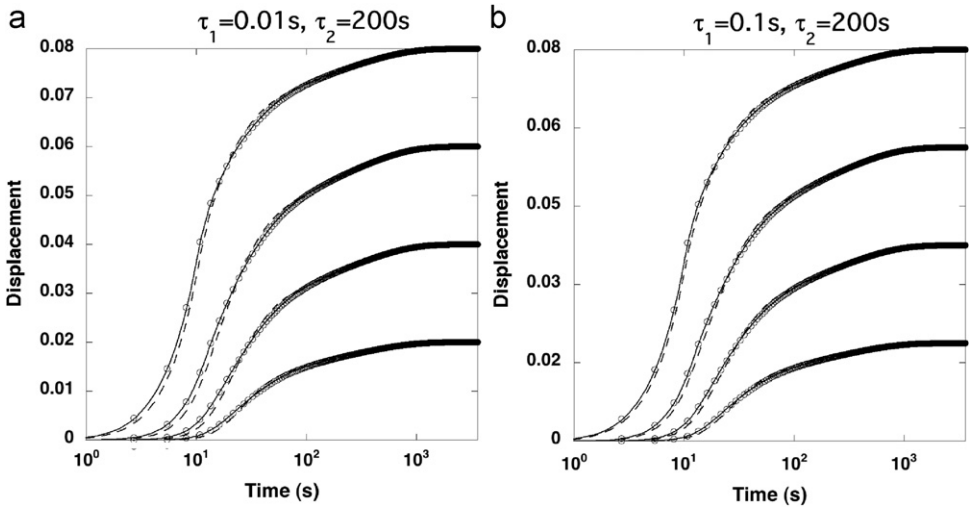

Fig. 3. Illustration of accuracy for displacement computations using the quadrature-based BPVE numerical method. The numerical solution in cases N_{int}=2 (dashed) and N_{int}=5 (solid) are compared to the theoretical solution (circles) at depths z/h=0.2, 0.4, 0.6, 0.8 [top to bottom] in the cases: (a) $\tau_1=0.01$ s, $\tau_2=200$ s and (b) $\tau_1=0.1$ s, $\tau_2=200$ s.

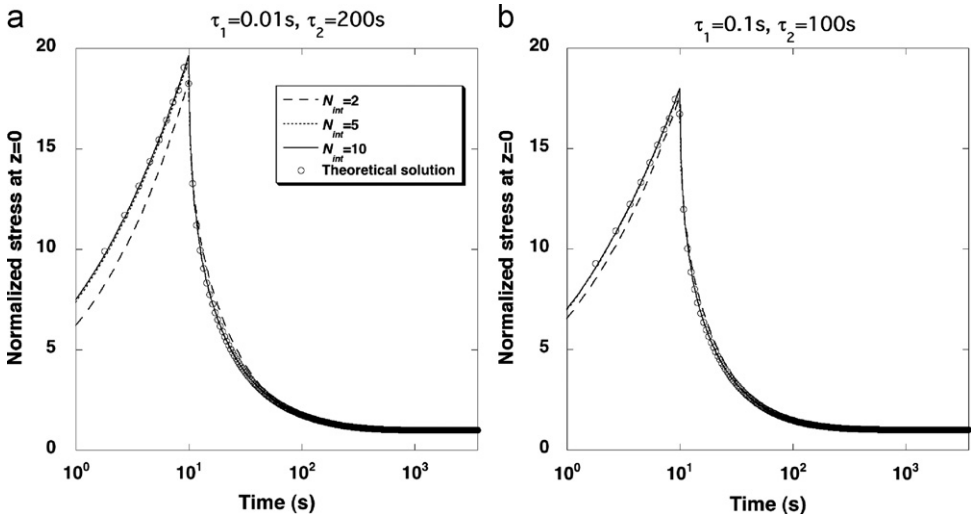

Fig. 4. Illustration of accuracy for surface stress computations using the quadrature-based BPVE numerical method. The numerical solution in cases N_{int}=2,5,10 are compared to the theoretical solution (circles) in the cases: (a) $\tau_1 = 0.01\,\mathrm{s}$, $\tau_2 = 200\,\mathrm{s}$ and (b) $\tau_1 = 0.1\,\mathrm{s}$, $\tau_2 = 100\,\mathrm{s}$.

error measure

$$E(t) \equiv |G^Q(t) - G(t)| = c\left|\sum_{j=1}^{N_{int}}\sum_{k=1}^{N_Q}\frac{l_j}{2}\frac{w_k}{s_{jk}}K_{jk}^Q(t)\,d\tau - \int_{\tau_1}^{\tau_2}\frac{e^{-t/s}}{s}\,ds\right|,$$
$$\text{for } t \in [0,\Delta t]. \tag{13}$$

Given Δt, $G(t)$ can be readily evaluated in terms of exponential integral functions on the domain $[0,\Delta t]$ for the nine cases considered, as demonstrated (in physical units) for the case $\Delta t = 0.25\,\mathrm{s}$ (Fig. 1). Values of $G(t)$ are then employed in $E(t)$ (13) to calibrate choices of N_{int} and N_Q for a given set of material and geometric parameters. We illustrate the process of calibrating N_{int} for the case N_Q=2 when t_f=3600 s and $\Delta t = 0.25\,\mathrm{s}$ in Fig. 2 for the cases with the largest ($\tau_1 = 0.01\,\mathrm{s}$, $\tau_2 = 200\,\mathrm{s}$) and smallest ($\tau_1 = 1.0\,\mathrm{s}$, $\tau_2 = 10\,\mathrm{s}$) errors. In the former case, with N_{int}=10, $E(t)$ ranged between 0.019 and 0.039 while $G(t)$ varied between 7.11 and 10.81 for a relative error of less than 0.55%. Similarly, in the latter case, with N_{int}=10, $E(t)$ ranged between 2.15×10^{-5} and 3.54×10^{-5} while $G(t)$ varied between 3.09 and 3.30 for a relative error of less than 0.0011%.

The quadrature-based numerical method (9), (10) and (12) was used to simulate the 1D confined compression stress relaxation problem (1)–(3) with a no-flux boundary condition (z=h) and a free-draining boundary (z=0). A ramp-and-hold displacement was prescribed as $u(0,t)$=$v_0 t$ for $0 < t < t_0$ and $u(0,t)$=$v_0 t_0$ for $t_0 < t \le t_f$ with t_0=10 s, v_0=h/10 and t_f=3600 s. Numerical parameters were taken as M=40, N_Q=2 and $\Delta t = 0.25\,\mathrm{s}$, representing a total of 14,400 time steps over the duration of the experiment. To assess accuracy, the number of quadrature intervals was varied as N_{int}=2,5,10. Prior to implementation, the governing equations were nondimensionalized, as described in Section 2.4. The numerical scheme was implemented in C++ and all computations were performed on a dual-2.8 GHz Quad Core Intel Xeon equipped Macintosh Pro computer.

Accuracy of the new scheme was assessed by comparison to a theoretical Laplace transform solution (Mak, 1986) Eqs. (24) and (25). Numerical inversion of Laplace transform representations was performed using a MATLAB implementation (Hollenbeck, 1998) of deHoog's algorithm (deHoog et al., 1982). In all cases, accuracy of computed displacements in the layer was excellent with N_{int}=5, and two representative cases are shown in Fig. 3. In general, accuracy of the numerical scheme improved as the difference between τ_1 and τ_2 decreased. Based on the displacement solution, a four-point finite difference approximation to the surface stress was also computed and compared with the theoretical solution. Stress responses were sensitive to τ_2 and two representative cases are shown in Fig. 4. Accuracy of the numerical scheme was very good in the case N_{int}=5 and excellent as N_{int} was increased to 10. For all cases considered in this study, numerical solutions on the domain [0 s, 3600 s] were obtained in less than one second.

4. Discussion

A new numerical method for the BPVE model of articular cartilage was developed based on a composite Gauss–Legendre quadrature approximation of the continuous spectrum relaxation function. The quadrature representation consists of a series of exponential terms and their separability property was exploited to develop a time discretization resulting in an update rule requiring retention of strain history at only the previous time step. This technique provides an alternate approach to approximating the continuous spectrum relaxation function using an exponential series that significantly enhances accuracy while minimizing computational cost. The method assigns coefficients and relaxation times in the exponential series based on the partition, abscissas and weights in the composite quadrature. For each case considered, accurate results were obtained in less than one second with the derived update rule yielding a computational cost proportional to N=14,400 time steps (i.e. when t_f=3600 s, $\Delta t = 0.25\,\mathrm{s}$). In contrast, the cost for direct solution of the full continuous spectrum numerical solution would be proportional to $N(N+1)/2 \approx 1 \cdot 10^8$ time steps.

The numerical method presented in this study will aid applications where material parameters in a BPVE cartilage model have fixed values or ranges, allowing for calibration of the quadrature technique to achieve the desired accuracy. While accuracy was demonstrated in the context of the 1D BPVE confined compression stress relaxation problem, all key aspects of the new method relate to the temporal discretization of the governing equations. The technique outlined in Section 2.3 is independent of the numerical method used for spatial discretization and can be extended to nonlinear strains. Consequently, we believe that our new quadrature-based temporal approximation scheme can significantly improve the accuracy and efficiency of finite element methods for the BPVE model of articular cartilage and such techniques will be considered in future studies by our group.

Conflict of interest statement

We, the authors of the manuscript entitled *A fast quadrature-based numerical method for the continuous spectrum biphasic poroviscoelastic model of articular cartilage* declare that there is no conflict of interest to report with respect to submission of this manuscript to the Journal of Biomechanics.

Acknowledgments

This work has been supported by funding from the National Science Foundation (DMS-0636590) and the National Institutes of Health (AG15768).

References

Desmarais, M., Aissaoui, R., 2008. Modeling of knee articular cartilage dissipation during gait analysis. Journal of Mechanics in Medicine and Biology 8, 377–394.

deHoog, F.R., Knight, J.H., Stokes, A.N., 1982. An improved method for numerical inversion of Laplace transforms. SIAM Journal on Scientific and Statistical Computing 3, 357–366.

DiSilvestro, M.R., Suh, J.K., 2001. Cross-validation study of the biphasic poroviscoelastic model of articular cartilage in unconfined compression, indentation and confined compression. Journal of Biomechanics 34, 519–525.

DiSilvestro, M.R., Suh, J.K., 2002. Biphasic poroviscoelastic characteristics of proteoglycan-depleted articular cartilage: simulation and degeneration. Annals of Biomedical Engineering 30, 792–800.

Fung, Y.C., 1993. Biomechanics Mechanical Properties of Living Tissues, second ed. Springer, New York.

Haider, M.A., Schugart, R.C., 2006. A numerical method for the continuous spectrum biphasic poroviscoelastic model of articular cartilage. Journal of Biomechanics 39, 177–183.

Hollenbeck, K.H., 1998. INVLAP.M: a matlab function for numerical inversion of Laplace transforms by the de Hoog algorithm. 〈http://www.mathtools.net/files/net/invlap.zip〉.

Mak, A.K., 1986. The apparent viscoelastic behavior of articular cartilage—the contributions from the intrinsic matrix viscoelasticity and interstitial fluid flows. Journal of Biomechanical Engineering 108, 123–130.

Mow, V.C., Kuei, S.C., Lai, W.M., Armstrong, C.G., 1980. Biphasic creep and stress relaxation of articular cartilage in compression: theory and experiments. Journal of Biomechanical Engineering 102, 73–84.

Neubert, H.K.P., 1963. A simple model representing internal damping in solid materials. Aeronautical Quarterly 14, 187–197.

Setton, L.A., Zhu, W., Mow, V.C., 1993. The biphasic poroviscoelastic behavior of articular cartilage: role of the surface zone in governing the compressive behavior. Journal of Biomechanics 26, 581–592.

Suh, J.K., Bai, S., 1998. Finite element formulation of biphasic poroviscoelastic model for articular cartilage. Journal of Biomechanical Engineering 120, 195–210.